The Many-Body Problem for Anisotropic Membrane Inclusions and the Self-Assembly of "Saddle" Defects into an "Egg Carton"

Paul G. Dommersnes* and Jean-Baptiste Fournier†
*Department of Physics, Norwegian University of Science and Technology, N-7491 Trondheim, Norway, and †Laboratoire de Physico-Chimie Théorique et FR CNRS 2438 "Matière et Systèmes Complexes," ESPCI, F-75231 Paris cedex 05, France

ABSTRACT We calculate the many-body, nonpairwise interaction between N rigid, anisotropic membrane inclusions by modeling them as point-like constraints on the membrane's curvature tensor and by minimizing the membrane's curvature energy. Because multipolar distortions of higher-order decay on very short distances, our calculation gives the correct elastic interaction energy for inclusions separated by distances of the order of several times their size. As an application, we show by thermally equilibrating the many-body elastic energy using a Monte Carlo algorithm, that inclusions shaped as "saddles" attract each other and build an "egg-carton" structure. The latter is reminiscent of some patterns observed in membranes obtained from biological extracts, the origin of which is still mysterious.

INTRODUCTION

Bilayer membranes, i.e., fluid sheets of lipids or surfactants with a fixed area and a bending rigidity (Safran, 1994; Seifert, 1997) often contain inclusions, either natural (proteins) (Lodish et al., 1995) or artificial (Dietrich et al., 1997; Koltover et al., 1999) that interact due to the membrane bending deformation they create (Goulian et al., 1993; Park and Lubensky, 1996; Dommersnes et al., 1998; Dommersnes and Fournier, 1999; Kim et al., 1998, 2000). These inclusions are often modeled as rigid disks that impose to the membrane, along their contour, a cone-angle (Goulian et al., 1993), or, more precisely, a contact-angle difference in the plane passing through the axis of the disk (see Fig. 1). The membrane is described as an infinite mathematical surface with a bending rigidity (Helfrich, 1973). For a membrane-embedded inclusion with a symmetry of revolution and a conical shape, the disk represents the cross-section of the inclusion and the cone angle accounts for the tilt of the surrounding lipid relative to the axis of the inclusion. Within this description, in which the membrane is treated as a structureless surface, only the long-range part of the interaction between the inclusions can be obtained. At very short distances (comparable to the membrane thickness $\simeq$4 nm), other short-range elastic interactions (Aranda-Espinoza et al., 1996; Fournier, 1999), electric and van der Waals interactions manifest themselves.

Calculating exactly the interaction between inclusions within the cone-angle model is a very heavy task, requiring multipoles expansions and the matching of the boundary conditions order by order (Goulian et al., 1993). Already to obtain the asymptotic interaction between two isotropic inclusions requires expanding up to fourth-order while minimizing with respect to the tilt β_0 of the disks (Fig. 1). To obtain more accurate results, one has to determine the multipoles coefficients numerically (Dommersnes et al., 1998), or devise approximation schemes (Kim et al., 1998).

In a coarse-grained description, i.e., in a description in which one is interested in the elastic interactions between inclusions that are separated by distances large with respect to their size, one can treat the inclusions as point-like objects, retaining only their lowest-order deformation "multipole." (Actually, because multipolar distortions of higher order decay on extremely short distances, it turns out that such calculations give accurate results even for inclusions separated by a few times their size.) What is then the point-like constraint equivalent to fixing the cone angle α at with the membrane meets the inclusion's cross section (Fig. 1)? In the absence of external forces, the height h_0 measuring the position of the inclusion above the reference plane is not constrained. On the contrary, it is freely optimized by minimization of the total membrane elastic free energy. Likewise, in the absence of external torques, the tilt β_0 of the inclusion relative to the reference plane is not con-

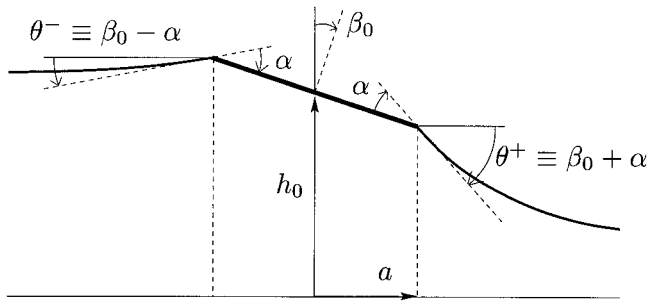

FIGURE 1 Section of a model membrane inclusion (*thick bar*), tilted by an angle β_0 with respect to the reference plane to which the membrane is parallel at infinity. The membrane (*curved line*) matches the inclusion with a cone angle α; the corresponding contact angles in the section's plane are θ^+ and θ^-. This model describes, for instance, a transmembrane protein with a conical shape.

Submitted September 21, 2001, and accepted for publication June 18, 2002.

Address reprint requests to J. B. Fournier, ESPCI, 10 rue Vauqelin, F-75231 Paris Cedex 05, France. E-mail: jbf@turner.pct.espci.fr.

0006-3495/02/12/2898/08 $2.00

strained (and in the presence of other inclusions, it is nonzero at equilibrium). Therefore, the membrane's contact angles, i.e., θ^+ and θ^- in the cross-section depicted in Fig. 1, are not imposed. What is actually imposed by the inclusion is the difference $\theta^+ - \theta^- \equiv 2\alpha$. The inclusion therefore imposes a difference of 2α in the membrane's inclination relative to the reference plane over a distance $2a$, i.e., a effective curvature $K = \alpha/a$. In a coarse-grained model in which the inclusions are described as point-like objects, modeling the inclusions in the way of Goulian et al. (1993) amounts to constraining pointwise the membrane curvature, while the membrane's height and tilt are unconstrained.

In this paper, we present a systematic way to calculate the elastic interaction between N membrane inclusions by imposing pointwise the membrane's curvature tensor. Using a Green function formalism, we determine the many-body, nonpairwise interaction by minimizing the membrane's bending energy while satisfying the point-like boundary conditions with the help of $3N$ Lagrange multipliers. This method gives the same mean-field results as obtained previously using a less transparent Gaussian path integral formalism (Dommersnes and Fournier, 1999). The present method overlooks the "Casimir" entropic fluctuation interaction. This is not so important because the fluctuation interaction becomes rapidly negligible with respect to the mean-field interaction when the prescribed curvatures of the inclusions increase (Dommersnes and Fournier, 1999). Finally, we show as an application, that a system of point-like "saddle" inclusions or defects, attract each other and self-assemble into a regular pattern that shapes the membrane into an "egg carton." This finding somehow corroborates the "hat and saddle" model proposed by Helfrich (1989) to explain the existence of corrugated membranes of biological origin (Helfrich and Mutz, 1988; Meyer et al., 1990).

INTERACTION BETWEEN *N* INCLUSIONS

For weak deformations $u(x, y)$ of the membrane with respect to a planar reference state (x, y), the membrane curvature energy takes the form (Helfrich, 1973)

$$F = \int \mathrm{d}^2 r \, \frac{\kappa}{2} (\nabla^2 u)^2, \tag{1}$$

to second order in u. Here κ is the membrane bending rigidity. The membrane's curvature is the second-rank tensor of components $u_{,\mathrm{xx}}$, $u_{,\mathrm{xy}}$, $u_{,\mathrm{yx}} = u_{,\mathrm{xy}}$, and $u_{,\mathrm{yy}}$. Here and in the following, the comma indicates spatial derivation. Note that only the trace of the tensor, $\nabla^2 u = u_{,\mathrm{xx}} + u_{,\mathrm{yy}}$ which is equal to twice the mean curvature, survives in F: the other first- or second-order scalars can be integrated by parts and give only boundary terms that vanish in an infinite membrane.

We consider N inclusions, at fixed positions $\mathbf{r}_\mathrm{i}$, each locally prescribing the two eigenvalues of the membrane curvature tensor (see the previous section). We also fix their orientation in the plane of the membrane. Therefore, each inclusion locally imposes all the components of the membrane curvature tensor. Hence, the vector $\mathbf{U}$ is prescribed,

$$\mathbf{U} = \begin{pmatrix} u_{,\mathrm{xx}}(\mathbf{r}_1) \\ u_{,\mathrm{xy}}(\mathbf{r}_1) \\ u_{,\mathrm{yy}}(\mathbf{r}_1) \\ \vdots \end{pmatrix}, \quad \mathbf{V}(r) = \begin{pmatrix} u_{,\mathrm{xx}}\delta(\mathbf{r} - \mathbf{r}_1) \\ u_{,\mathrm{xy}}\delta(\mathbf{r} - \mathbf{r}_1) \\ u_{,\mathrm{yy}}\delta(\mathbf{r} - \mathbf{r}_1) \\ \vdots \end{pmatrix}. \tag{2}$$

The vector $\mathbf{V}$ has been introduced for further use. The dots indicate that the three components written down should be repeated for $\mathbf{r}_2, \ldots, \mathbf{r}_\mathrm{N}$. The vector $\mathbf{U}$ has $3N$ components U_α. The constraints sets by the inclusions can be written as

$$U_\alpha = K_\alpha, \quad (\alpha = 1, \ldots, 3N), \tag{3}$$

where the K_α are the prescribed curvature components.

Introducing $3N$ Lagrange multipliers Λ_α, the equilibrium shape of the membrane is obtained by minimizing the functional

$$F^* = \kappa \int \mathrm{d}^2 r \left[\frac{1}{2} (\nabla^2 u)^2 - \Lambda_\alpha V_\alpha(\mathbf{r}) \right], \tag{4}$$

where summation over repeated indices is implied. The vector $\mathbf{V}(\mathbf{r})$ is defined in Eq. 2; the δ are Dirac delta functions. Considering a variation of the membrane shape $u(\mathbf{r}) \rightarrow u(\mathbf{r}) + \delta u(\mathbf{r})$, the first-order variation of F^* is

$$\delta F^* = \kappa \int \mathrm{d}^2 r \, [\delta u \nabla^4 u - \Lambda_\alpha \delta V_\alpha(\mathbf{r})], \tag{5}$$

$$= \kappa \int \mathrm{d}^2 r \, [\nabla^4 u - \Lambda_\alpha D_\alpha(\mathbf{r})] \delta u, \tag{6}$$

where transformations using integrations by parts were used. The operator $\nabla^4 = \nabla^2 \nabla^2$ is the bi-Laplacian operator. The vector $\mathbf{D}$ has the components,

$$\mathbf{D}(\mathbf{r}) = \begin{pmatrix} \delta_{,\mathrm{xx}}(\mathbf{r} - \mathbf{r}_1) \\ \delta_{,\mathrm{xy}}(\mathbf{r} - \mathbf{r}_1) \\ \delta_{,\mathrm{yy}}(\mathbf{r} - \mathbf{r}_1) \\ \vdots \end{pmatrix}, \tag{7}$$

where the dots indicate again repetition for $\mathbf{r}_2, \ldots, \mathbf{r}_\mathrm{N}$. Because, at equilibrium, δF^* must vanish for all δu, the membrane's equilibrium equation is

$$\nabla^4 u = \Lambda_\alpha D_\alpha(\mathbf{r}). \tag{8}$$

Let us now introduce the Green function of the operator ∇^4, i.e., the solution of $\nabla^4 G(\mathbf{r}) = \delta(\mathbf{r})$, which is

$$G(\mathbf{r}) = \frac{1}{16\pi} r^2 \ln r^2. \tag{9}$$

Because of the linearity of the problem, the solution of Eq. 8 is

$$u(\mathbf{r}) = \Lambda_\alpha G_\alpha(\mathbf{r}), \tag{10}$$

where the vector $\mathbf{G}(\mathbf{r})$ is defined by

$$\mathbf{G}(\mathbf{r}) = \begin{pmatrix} G_{,xx}(\mathbf{r}-\mathbf{r}_1) \\ G_{,xy}(\mathbf{r}-\mathbf{r}_1) \\ G_{,yy}(\mathbf{r}-\mathbf{r}_1) \\ \vdots \end{pmatrix}. \tag{11}$$

Our last task is to relate the Lagrange multipliers Λ_α to the actual constraints K_α. Eq. 3 can be rewritten as

$$\mathcal{L}_\alpha u = K_\alpha, \tag{12}$$

where $\mathcal{L}$ is the vector of operators

$$\mathcal{L} = \begin{pmatrix} \partial_x^2|_{\mathbf{r}_1} \\ \partial_x\partial_y|_{\mathbf{r}_1} \\ \partial_y^2|_{\mathbf{r}_1} \\ \vdots \end{pmatrix}. \tag{13}$$

Then, from Eqs. 10 and 12, we have $\mathcal{L}_\alpha(\Lambda_\beta G_\beta) = K_\alpha$, which can be rewritten as $(\mathcal{L}_\alpha G_\beta)\Lambda_\beta = K_\alpha$. Hence, introducing the $3N \times 3N$ matrix $\mathbf{M}$ with elements

$$M_{\alpha\beta} = \mathcal{L}_\alpha G_\beta, \tag{14}$$

we obtain

$$\Lambda_\alpha = M^{-1}_{\alpha\beta} K_\beta. \tag{15}$$

At this point, we have formally solved the problem. Knowing the positions of the inclusions, we can calculate the matrix $\mathbf{M}$. Then, given the prescribed curvatures K_α, we obtain the Λ_α from Eq. 15. Using Eq. 10, we deduce the membrane shape,

$$u(\mathbf{r}) = M^{-1}_{\alpha\beta} G_\alpha(\mathbf{r}) K_\beta. \tag{16}$$

Interaction energy

Integrating Eq. 1 by parts yields

$$F = \frac{\kappa}{2}\int \mathrm{d}^2 r\, u\nabla^4 u = \frac{\kappa}{2}\Lambda_\alpha \int \mathrm{d}^2 r\, u D_\alpha(\mathbf{r}). \tag{17}$$

Integrating this result by parts again, then making use of the boundary conditions (thanks to the Dirac distribution), we obtain $F = \frac{1}{2}\kappa\Lambda_\alpha K_\alpha$, i.e.,

$$F = \tfrac{1}{2}\kappa M^{-1}_{\alpha\beta} K_\alpha K_\beta. \tag{18}$$

Structure of the interaction matrix

The matrix $\mathbf{M}$ has the structure,

$$\mathbf{M} = \begin{pmatrix} m_{11} & m_{12} & \dots & m_{1N} \\ m_{21} & m_{22} & & \vdots \\ \vdots & & \ddots & \vdots \\ m_{N1} & \dots & \dots & m_{NN} \end{pmatrix}, \tag{19}$$

where, according to Eq. 14, the m_{ij} are the N^2 matrices of size 3×3, defined by

$$m_{ij} = \begin{pmatrix} G_{,xxxx}(\mathbf{r}_i-\mathbf{r}_j) & G_{,xxxy}(\mathbf{r}_i-\mathbf{r}_j) & G_{,xxyy}(\mathbf{r}_i-\mathbf{r}_j) \\ G_{,xxxy}(\mathbf{r}_i-\mathbf{r}_j) & G_{,xxyy}(\mathbf{r}_i-\mathbf{r}_j) & G_{,xyyy}(\mathbf{r}_i-\mathbf{r}_j) \\ G_{,xxyy}(\mathbf{r}_i-\mathbf{r}_j) & G_{,xyyy}(\mathbf{r}_i-\mathbf{r}_j) & G_{,yyyy}(\mathbf{r}_i-\mathbf{r}_j) \end{pmatrix}. \tag{20}$$

Setting

$$\mathbf{r}_i - \mathbf{r}_j = \rho_{ij}\cos\theta_{ij}\,\hat{\mathbf{x}} + \rho_{ij}\,sin\,\theta_{ij}\,\hat{\mathbf{y}} \tag{21}$$

yields explicitely

$$m_{ij} = \frac{1}{4\pi\rho_{ij}^2}\begin{pmatrix} \cos(4\theta_{ij}) - 2\cos(2\theta_{ij}) & \sin(2\theta_{ij})[2\cos(2\theta_{ij}) - 1] & -\cos(4\theta_{ij}) \\ \sin(2\theta_{ij})[2\cos(2\theta_{ij}) - 1] & -\cos(4\theta_{ij}) & -\sin(4\theta_{ij}) - \sin(2\theta_{ij}) \\ -\cos(4\theta_{ij}) & -\sin(4\theta_{ij}) - \sin(2\theta_{ij}) & \cos(4\theta_{ij}) + 2\cos(2\theta_{ij}) \end{pmatrix}. \tag{22}$$

Because m_{ij} diverges when $i = j$, it is necessary to regularize the Green function at short distances, e.g., by introducing a high wave-vector cutoff. Indeed Eq. 1 only describes correctly the membrane elastic energy for wavevectors $q \lesssim \Lambda$, where Λ^{-1} is of the order of the membrane thickness. Adding a high wave-vector cutoff actually mimics the effect of the higher-order derivatives that have been omitted in the free energy functional. The precise way to regularize is not important because the interaction energy turns out to be insensitive to the detail of the regularization for inclusions separations larger than a few time the inclusions size. In other words, the regularization scheme rather affects the self-energy present in Eq. 18 than the interaction energy.

From the definition of the Green function $G(\mathbf{r})$, we deduce

$$G_{,xxxx}(\mathbf{r}) = \int \frac{\mathrm{d}^2 q}{(2\pi)^2}\frac{q_x^4 e^{i\mathbf{q}\cdot\mathbf{r}}}{q^4}, \tag{23}$$

with $q_x^3 q_y$ instead of q_x^4 for $G_{,xxxy}(r)$, with $q_x^2 q_y^2$ for $G_{,xxyy}(r)$, and so on. Hence, introducing the cutoff, we obtain

$$G_{,xxxx}(\mathbf{0}) = \int_0^{\Lambda} \frac{q\,\mathrm{d}q}{(2\pi)^2} \int_0^{2\pi} \mathrm{d}\theta \cos^4\theta = \frac{3\Lambda^2}{32\pi}, \quad (24)$$

and so forth. With the above prescription, we obtain, therefore

$$m_{ij} = \frac{\Lambda^2}{32\pi} \begin{pmatrix} 3 & 0 & 1 \\ 0 & 1 & 0 \\ 1 & 0 & 3 \end{pmatrix}, \quad \text{for } i = j. \quad (25)$$

Interaction between two identical isotropic inclusions

Without loss of generality, we place the two inclusions on the x-axis at a separation R. Then, with $\mathbf{r}_1 - \mathbf{r}_2 = R\hat{\mathbf{x}}$, we obtain the matrix $\mathbf{M}$,

$$\mathbf{M} = \frac{\Lambda^2}{32\pi} \begin{pmatrix} 3 & 0 & 1 & -8\epsilon^2 & 0 & -8\epsilon^2 \\ 0 & 1 & 0 & 0 & -8\epsilon^2 & 0 \\ 1 & 0 & 3 & -8\epsilon^2 & 0 & 24\epsilon^2 \\ -8\epsilon^2 & 0 & -8\epsilon^2 & 3 & 0 & 1 \\ 0 & -8\epsilon^2 & 0 & 0 & 1 & 0 \\ -8\epsilon^2 & 0 & 24\epsilon^2 & 1 & 0 & 3 \end{pmatrix}, \quad (26)$$

where $\epsilon = \Lambda^{-1}/R$. For two identical isotropic inclusions, each prescribing a diagonal curvature tensor with modulus K, we set

$$\mathbf{K}^t = (K, 0, K, K, 0, K), \quad (27)$$

where the superscript t means transpose. We obtain from Eq. 18 the interaction energy,

$$F = \frac{512\pi\kappa(K/\Lambda)^2}{(R\Lambda)^4 + 8(R\Lambda)^2 - 32} = 8\pi\kappa\alpha^2\left(\frac{a}{R}\right)^4 + \mathbb{O}\left(\frac{1}{R^6}\right), \quad (28)$$

in which we have discarded a constant term. In the second expression in Eq. 28, we have set $K = \alpha/a$, where α is the cone angle imposed by the inclusions (see Fig. 1) and $\Lambda = 2/a$, in agreement with Park and Lubensky (1996). We thus recover exactly the asymptotic result of Goulian et al. (1993), which was obtained from multipolar expansions, and in which a was the radius of the disks modeling the inclusions. In other words, the correspondence $\Lambda = 2/a$ allows matching of the present results, obtained from the pointwise model, with the results obtained by multipolar expansions for inclusions of finite size.

It should be noted that the interaction given by Eq. 28 is exact within the present formalism (for r larger than a few times the cutoff Λ^{-1}), whereas multipolar expansions can only give, in analytical form, the leading asymptotic orders. Indeed, one of us checked, by numerically calculating the multipolar expansion with a large number of multipoles, that, for the cone-angle model, the exact interactions up to distances of the order of several times the inclusion radius closely follows Eq. 28 (P. Galatola and J.-B. Fournier, unpublished result).

Interaction between two purely anisotropic inclusions

To calculate the interaction between two purely anisotropic inclusions, i.e., two inclusions imposing each two opposite eigenvalues of the curvature tensor (K and $-K$), we set

$$\mathbf{K}^t = (K\cos 2\theta_1, K\sin 2\theta_1, -K\cos 2\theta_1, K\cos 2\theta_2, K\sin 2\theta_2, -K\cos 2\theta_2). \quad (29)$$

The first inclusion is rotated by an angle θ_1 with respect to the x-axis and the second one by an angle θ_2. Such inclusions could be proteins having a conical section of angle $\alpha = Ka$ with the apex downward in one of the two sagittal sections and a conical section of angle $-\alpha$ with the apex upward in the perpendicular sagittal section. The interaction, given by Eqs. 18, 26, and 29, is now

$$F = -16\pi\kappa\theta^2 \cos[2(\theta_1 + \theta_2)]\left(\frac{a}{R}\right)^2 + \mathbb{O}\left(\frac{1}{R^4}\right), \quad (30)$$

where we have used again the correspondence $a = 2\Lambda^{-1}$ (see previous section). It decays as $1/R^2$, hence it is of longer range than the interaction between two isotropic inclusions (decaying as $1/R^4$). Furthermore, it is attractive when the two inclusions have their axes of same nature oriented parallel, whereas two isotropic inclusions always repel one another.

Interaction between *N* point-like inclusions of arbitrary shapes

It is straightforward, within the present formalism, to analytically calculate the total interaction between N inclusions, each locally setting the membrane's curvature tensor. Note that, although the inclusions are treated as points, the total energy is nonpairwise additive. The solution for N inclusions is not the superposition of the individual solutions because of the requirement of strictly matching the boundary conditions on every inclusion. An illustration of the many-body effect is given in the Appendix. To calculate the interaction given the positions of the inclusions, one first determines the matrix $\mathbf{M}$ using Eqs. 19, 22, and 25. It is then necessary to invert this $3N \times 3N$ matrix (or at least to solve numerically the linear system yielding the Lagrange multipliers). This can be easily done numerically. One builds then the vector $\mathbf{K}$ that contains the curvature tensor's components $u_{,xx}$, $u_{,xy}$, $u_{,yy}$ set by the inclusions. The latter are

placed as in the vector **U** of Eq. 2. Note that **K** depends on the orientations of the inclusions. The interaction energy is eventually obtained from Eq. 18.

The many details of this interaction, for two or more inclusions of arbitrary shapes, and the strength of the nonpairwise contributions relative to the pairwise ones, is outside of the scope of this paper and will be discussed in a review paper elsewhere.

AGGREGATION OF AN ASSEMBLY OF SADDLE INCLUSIONS INTO AN EGG-CARTON STRUCTURE

According to the result of the previous section, we expect that a collection of purely anisotropic inclusions will aggregate. However, due to the many-body character of the elastic interaction and because of the thermal fluctuations, it is not obvious whether they will build a regular pattern or a disordered one. To study this collective behavior, we have considered a system of $N = 121$ purely anisotropic inclusions with a cone angle $\alpha \simeq 15°$, living in a membrane with $\kappa \simeq 60\ k_BT$ (Song and Waugh, 1993; Strey et al., 1995). This corresponds to the dimensionless parameter $(\kappa/k_BT)^{1/2}K\Lambda^{-1} \simeq 1$. We start by placing the inclusions at random positions and orientations. The total elastic energy of the system is calculated as explained in the previous section. The contribution of the short-range interactions is taken into account in the simplest way by adding a hard core of radius r_0. For definiteness, we chose $r_0 = 4\Lambda^{-1}$, assuming that the size of the inclusions was somewhat larger than the membrane thickness.

To determine the equilibrium configuration of this system of inclusions at temperature T, we perform Monte Carlo simulations. At each Monte Carlo step, we try a move consisting of either a translation or a rotation of one arbitrarily chosen inclusion, and we test the energy variation against k_BT according to the standard Metropolis algorithm (Metropolis et al., 1953; Frenkel and Smit, 1996). The amplitude of the moves is adjusted to keep an average acceptance rate of 50%. We let the system equilibrate using $\simeq 10^7$ Monte Carlo steps. We find that the inclusions attract each other, and most interestingly, that the equilibrium membrane shape (calculated according to Eq. 16) displays an undulated shape in the form of an egg carton (Fig. 2).

The structure displayed in Fig. 2 is a square lattice. To assess that this corresponds to an equilibrium state and to compute the value of the lattice parameter, we use the following procedure. We build a square lattice of inclusions parallel to the (x, y) reference frame. According to the typical snapshots obtained in the Monte Carlo simulations, we initially orient the inclusions in such a way that their axes of smallest curvature are alternatively at 45° and −45° with respect to the x-axis. Then, we run the Monte Carlo simulation, and, after it has equilibrated, we compute the pair correlation function $g(X, Y)$. To calculate the latter, we choose at the very beginning one particular inclusion, labeled i_0, and its first neighbor on the right of the x-axis, labeled i_1. Because, during the Monte Carlo simulation, the lattice drifts and rotates, we define a dynamic frame (X, Y) centered on inclusion i_0 with the X axis passing through inclusion i_1. Then, we calculate the average density of inclusions at point (X, Y). To define the pair correlation function $g(X, Y)$, we normalize this function to unity at the origin. The result is that $g(X, Y)$ displays a regular square pattern of pics, which demonstrates that the square lattice is stable. From the plot of $g(0, Y)$, shown in Fig. 3, we deduce the lattice parameter $b \simeq 8.5\Lambda^{-1}$. The fact that this value is just larger than twice the hard-core radius $r_0 = 4\Lambda^{-1}$ demonstrates that the inclusions tend to aggregate as much as possible and that the short range interactions actually fix the lattice periodicity.

We have thus shown that purely anisotropic inclusions locally imposing a saddle-like deformation aggregate into a pattern that shapes the membrane into an egg carton. However, because it is the short-range interaction that actually defines the equilibrium pattern, we should keep in mind that more realistic short-range interactions could modify both the value of the lattice parameter and the symmetry of the lattice.

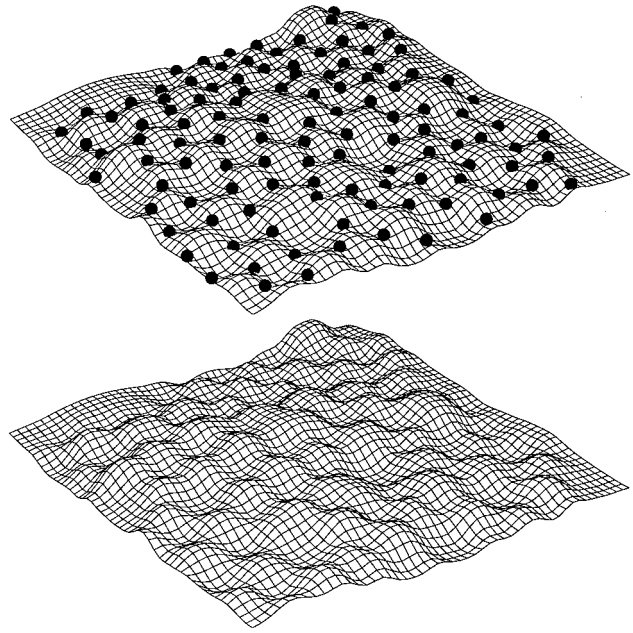

FIGURE 2 Typical snapshot of the equilibrium configuration for $N = 121$ identical anisotropic inclusions obtained by a Monte Carlo simulation. Each inclusion locally imposes two opposite eigenvalues of the membrane's curvature tensor (K and $-K$), corresponding to a cone angle $\simeq 15°$. The membrane bending rigidity is $\kappa \simeq 60\ k_BT$. Only the region where the inclusions are aggregated is displayed (the membrane is actually infinite in the calculation). *Top*, Equilibrium configuration: the inclusions, shown as black dots, are actually oriented parallel to the axes of the local saddles in which they sit. *Bottom*, The same configuration with the inclusions hidden to better evidence the egg-carton structure.

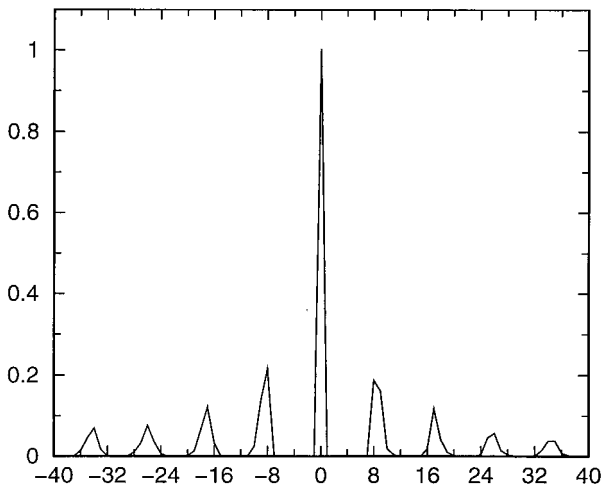

FIGURE 3 Pair correlation function along an axis of the egg-carton lattice. The parameters are the same as in Fig. 2.

POSSIBLE RELATIONSHIP WITH THE EXPERIMENTALLY OBSERVED EGG-CARTONS SUPERSTRUCTURES OF MEMBRANES

There is evidence that membrane superstructure may occur in biomembranes. Modulated structures displaying an egg carton-like shape with a square symmetry have been observed by freeze–fracture electron microscopy in the membranes of *L* form (wall-less) cells of *Streptomyces hygroscopicus* and in reconstituted bilayers formed with lipid extracts (Sternberg et al., 1986, 1987; Meyer et al., 1990). The egg carton appeared under gel phase conditions also near to the transition from the fluid state (Meyer et al., 1998; Meyer and Richter, 2001) (see Fig. 4). Another reason for postulating the existence of such superstructures is some evidence of anomalous membrane roughness suggested by studies of membrane adhesion (Servuss and Helfrich, 1989). Recent experiments using cryo-transmission electron microscopy on dilute vesicle dispersions have also shown the formation of disordered superstructures in fluid dioleoyl-phosphatidylcholine membranes (Klösgen and Helfrich, 1997).

It was theoretically proposed by Helfrich (1989) that extrinsic or intrinsic saddle "defects" might aggregate into ordered arrays and produce egg-carton superstructures. Alternatively, higher-order terms in the membrane elasticity were proposed to yield disordered egg-carton structures (Goetz and Helfrich, 1996). Other models have suggested that a nematic-like order of the polar heads of the lipids might locally favor saddle-shaped regions and egg-carton structures (Fournier, 1996). Indeed, as mentioned in the paper by Meyer et al. (1990), egg cartons have been seen in mixtures of egg yolk phosphatidylcholine and bacterial cardiolipin in the presence of Ca^{2+} ions (micrograph in Meyer and Richter, 2001, Fig. 14d). Cardiolipins have elongated polar heads, which, when bridged by the calcium ions, might develop a nematic order (suggestion of V. Norris, Université de Rouen, France). At the present time, it is not known whether saddle-shaped regions are responsible for the formation of egg cartons and what the origin of these saddle regions might be. Possible candidates are instabilities due to higher-order elastic terms, anisotropic lipid associations coupling with the membrane curvature, or hydration-induced packing frustration between both monolayers (H. W. Meyer, private communication).

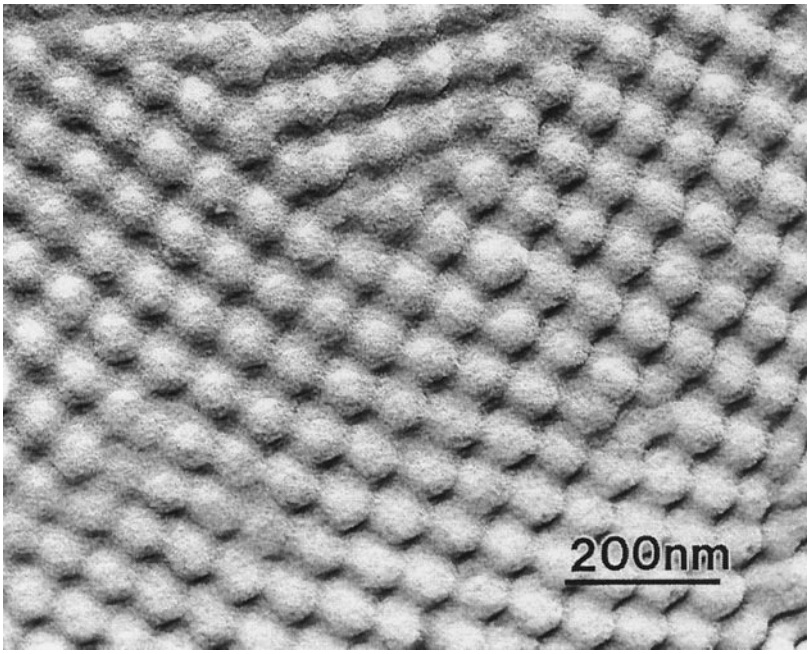

FIGURE 4 Orthogonally arranged egg-carton pattern of ~74 nm repeat distance in hydrated phospholipids extracted from *Streptomyces hygroscopicus L33-354* stable *L*-form cells grown at 28°C. Phospholipid dispersion with 90% [w/w] water content (distilled water) stored several days at 4°C, heated to 12°C, and frozen from this temperature for freeze–fracturing. (Courtesy W. Richter.)

What the present paper shows is that saddle-like regions, whatever their origin, indeed attract each other under the influence of long-range elastic forces and aggregate into an egg-carton structure. Our calculations therefore corroborates the suggestion of Helfrich (1989). Note that our coarse-grained model actually makes no hypothesis concerning the origin of the saddle-like inclusions. We presented the calculations having in mind anisotropic transmembrane proteins. However, any mechanism inducing a local curvature constraint with a saddle-like symmetry should yield the same effect. The specificities would be in the short-range interactions. Our calculations showed that, for nonspecific repulsive short-range interactions, the lattice parameter of the egg-carton superstructure compares with the dimensions of the saddle-like inclusions. Therefore, it is not possible, without knowing the nature of the saddle-like actors, to compare the experimentally observed lattice spacings with the calculated ones. This suggests however, because experiments on different systems have reported lattice spacing ranging from 4 nm (Klösgen and Helfrich, 1997) to 75 nm (Meyer et al., 1990), that the possible saddle-like defects involved might have different origins.

CONCLUSION

In conclusion, we have devised a powerful method to calculate the many-body interaction between N inclusions of arbitrary shape. We model the inclusions as point-like constraints on the membrane curvature tensor while the membrane is treated as a surface with a bending rigidity. Being coarse-grained, this model can apply to any intrinsic or extrinsic source of local curvature (e.g., transmembrane proteins, membrane binding cytosol proteins, locally stressed membrane regions, phase-separated regions with an orientational order, etc.). Our model is the exact point-like equivalent of the cone-angle model of Goulian et al. (1993). In agreement with previous statistical mechanics calculations (Dommersnes and Fournier, 1999), we have found that purely anisotropic inclusions (i.e., inclusions imposing opposite eigenvalues of the curvature tensor) attract each other with a potential that decays as $1/R^2$ where R is the separation between the inclusions. We showed that these inclusions aggregate into a pattern that shapes the membrane into an egg carton. This corroborates Helfrich's (1989) suggestion that experimentally observed egg-carton superstructures might result from the cooperative association of saddle-like defects.

APPENDIX: MANY-BODY EFFECT

By way of illustration, let us determine the many-body contribution to the interaction energy for three identical isotropic inclusions on an equilateral triangle. We place inclusion 1 on the x-axis and inclusions 2 and 3 on the y-axis, the sequence 1, 2, 3 making a counterclockwise rotation. Let R be the distance between any two inclusions. Using the formalism of Structure of the Interaction Matrix, with $\theta_{12} = -\pi/6$, $\theta_{13} = \pi/6$, and $\theta_{23} = \pi/2$, the interaction matrix is given by

$$\mathbf{M} = \frac{\Lambda^2}{32\pi}\begin{pmatrix} 3 & 0 & 1 & -12\epsilon^2 & 0 & 4\epsilon^2 & -12\epsilon^2 & 0 & 4\epsilon^2 \\ 0 & 1 & 0 & 0 & 4\epsilon^2 & 8\sqrt{3}\epsilon^2 & 0 & 4\epsilon^2 & -8\sqrt{3}\epsilon^2 \\ 1 & 0 & 3 & 4\epsilon^2 & 8\sqrt{3}\epsilon^2 & 4\epsilon^2 & 4\epsilon^2 & -8\sqrt{3}\epsilon^2 & 4\epsilon^2 \\ -12\epsilon^2 & 0 & 4\epsilon^2 & 3 & 0 & 1 & 24\epsilon^2 & 0 & -8\epsilon^2 \\ 0 & 4\epsilon^2 & 8\sqrt{3}\epsilon^2 & 0 & 1 & 0 & 0 & -8\epsilon^2 & 0 \\ 4\epsilon^2 & 8\sqrt{3}\epsilon^2 & 4\epsilon^2 & 1 & 0 & 3 & -8\epsilon^2 & 0 & -8\epsilon^2 \\ -12\epsilon^2 & 0 & 4\epsilon^2 & 24\epsilon^2 & 0 & -8\epsilon^2 & 3 & 0 & 1 \\ 0 & 4\epsilon^2 & -8\sqrt{3}\epsilon^2 & 0 & -8\epsilon^2 & 0 & 0 & 1 & 0 \\ 4\epsilon^2 & -8\sqrt{3}\epsilon^2 & 4\epsilon^2 & -8\epsilon^2 & 0 & -8\epsilon^2 & 1 & 0 & 3 \end{pmatrix}, \tag{A1}$$

where again $\epsilon = \Lambda^{-1}/R$. We then set $\mathbf{K}^t = (K, 0, K, K, 0, K, K, 0, K)$ and the interaction is given by Eq. 18. With, as previously, $K = \alpha/a$ and $\Lambda = 2/a$, we obtain

$$F_3 = 12\pi\kappa\alpha^2\left(\frac{a}{R}\right)^4 + \mathbb{O}\left(\frac{1}{R^6}\right). \tag{A2}$$

We need to compare this result with three times the pairwise interaction for two isotropic inclusions. Because the prefactor in Eq. 28 is 8, assuming pairwise interactions would yield a prefactor of 24 instead of the value of 12 obtained above. Therefore the many-body effect reduces the interaction by 50%.

The authors are indebted to H. W. Meyer and W. Richter for helpful discussions and for providing the picture of Fig. 4. P.G.D. acknowledges support from the Research Council of Norway under grant no. 134996/432.

REFERENCES

Aranda-Espinoza, H., A. Berman, N. Dan, P. Pincus, and S. A. Safran. 1996. Interaction between inclusions embedded in membranes. *Biophys. J.* 71:648–656.

Dietrich, C., M. Angelova, and B. Pouligny. 1997. Adhesion of latex spheres to giant phospholipid vesicles: statics and dynamics. *J. Phys. France.* 7:1651–1682.

Dommersnes, P. G., J.-B. Fournier, and P. Galatola. 1998. Long-range elastic forces between membrane inclusions in spherical vesicles. *Europhys. Lett.* 42:233–238.

Dommersnes, P. G., and J.-B. Fournier. 1999. *N*-body study of anisotropic membrane inclusions: membrane mediated interactions and ordered aggregation. *Eur. Phys. J. B.* 13:9–12.

Fournier, J.-B. 1996. Non-topological saddle-splay and curvature instabilities from anisotropic membrane inclusions. *Phys. Rev. Lett.* 76: 4436–4439.

Fournier, J.-B. 1999. Microscopic membrane elasticity and interactions among membrane inclusions: interplay between the shape, dilation, tilt and tilt-difference modes. *Eur. Phys. J. B.* 11:261–272.

Frenkel, D., and B. Smit. 1996. Understanding Molecular Simulation. Academic Press, New York.

Goetz, R., and W. Helfrich. 1996. The egg carton: theory of a periodic superstructure of some lipid membranes. *J. Phys. II France.* 6:215–223.

Goulian, M., R. Bruinsma, and P. Pincus. 1993. Long-range forces in heterogeneous fluid membranes. *Europhys. Lett.* 22:145–150.

Helfrich, W. 1973. Elastic properties of lipid bilayers: theory and possible experiments. *Z. Naturforsch. C.* 28:693–703.

Helfrich, W. 1989. Hats and saddles in lipid membranes. *Liquid Cryst.* 5:1647–1658.

Helfrich, W., and M. Mutz. 1988. Unbinding transition and mutual adhesion in general of DGDG membranes. *In* Fluctuations and Pattern Growth: Experiments and Theory. H. E. Stanley and N. Ostrowsky, editors. Kluwer, Dordrecht, The Netherlands. 222–226.

Kim, K. S., J. Neu, and G. Oster. 1998. Curvature-mediated interactions between membrane proteins. *Biophys. J.* 75:2274–2291.

Kim, K. S., J. Neu, and G. Oster. 2000. Effect of protein shape on multibody interactions between membrane inclusions. *Phys. Rev. E.* 61:4281–4285.

Klösgen, B., and W. Helfrich. 1997. Cryo-transmission electron microscopy of a superstructure of fluid dioleoylphosphatidylcholine (DOPC) membranes. *Biophys. J.* 73:3016–3029.

Koltover, I., J. O. Rädler, and C. S. Safinya. 1999. Membrane mediated attraction and ordered aggregation of colloidal particles bound to giant phospholipid vesicles. *Phys. Rev. Lett.* 82:1991–1994.

Lodish, H., D. Baltimore, A. Berk, S. L. Zipursky, P. Matsudaira, and J. Darnel. 1995. Molecular Cell Biology. Scientific American Books, New York.

Metropolis, N., A. W. Rosenbluth, M. N. Rosenbluth, A. H. Teller, and E. Teller. 1953. Equation of state calculation by east computing machines. *J. Chem. Phys.* 21:1087–1091.

Meyer, H. W., W. Richter, and J. Gumpert. 1990. Periodically curved bilayer structures observed in hyphal cells or stable L-form cells of a *Streptomyces* strain, and in liposomes formed by the extracted lipids. *Biochim. Biophys. Acta.* 1026:171–178.

Meyer, H. W., M. Westermann, M. Stumpf, W. Richter, A. S. Ulrich, and C. Hoischen. 1998. Minimal radius of curvature of lipid bilayers in the gel phase state corresponds to the dimension of biomembrane structures "caveolae". *J. Struct. Biol.* 124:77–87.

Meyer, H. W., and W. Richter. 2001. Freeze–fracture studies on lipids and membranes. *Micron.* 32:615–644.

Park, J. M., and T. C. Lubensky. 1996. Interactions between membrane inclusions on fluctuating membranes. *J. Phys. I France.* 6:1217–1235.

Safran, S. A. 1994. Statistical Thermodynamics of Surfaces, Interfaces and Membranes. Addison-Wesley, Reading, MA.

Song, J., and R. E. Waugh. 1993. Bending rigidity of SOPC membranes containing cholesterol. *Biophys. J.* 64:1967–1970.

Seifert, U. 1997. Configurations of fluid membranes and vesicles. *Adv. Phys.* 46:13–177.

Servuss, R. M., and W. Helfrich. 1989. Mutual adhesion of lecithin membranes at ultralow tensions. *J. Phys.* 50:809–827.

Sternberg, B., J. Gumpert, H. W. Meyer, and G. Reinhardt. 1986. Structures of liposome membranes as models for similar features of cytoplasmic membranes of bacteria. *Acta Histochem.* 145:139–145.

Sternberg, B., J. Gumpert, G. Reinhardt, and K. Gawrisch. 1987. Electron microscopic and biophysical studies of liposome membrane structures characterize similar features of the membranes of *Streptomyces hygroscopicus*. *Biochim. Biophys. Acta.* 898:223–230.

Strey, H., M. Peterson, and E. Sackmann. 1995. Measurement of erythrocyte membrane elasticity by flicker eigenmode decomposition. *Biophys. J.* 69:478–488.